RESEARCH ARTICLE

The cytochrome P450 CYP77A4 is involved in auxin-mediated patterning of the *Arabidopsis thaliana* embryo

Kensuke Kawade[1,2,3,4,*,‡,§], Yimeng Li[4,‡], Hiroyuki Koga[5], Yuji Sawada[4], Mami Okamoto[4], Ayuko Kuwahara[4], Hirokazu Tsukaya[1,5,*] and Masami Yokota Hirai[4,§]

ABSTRACT

Metabolism often plays an important role in developmental control, in addition to supporting basal physiological requirements. However, our understanding of this interaction remains limited. Here, we performed quantitative phenome analysis of *Arabidopsis thaliana* cytochrome P450 mutants to identify a novel interaction between development and metabolism. We found that *cyp77a4* mutants exhibit specific defects in cotyledon development, including asymmetric positioning and cup-shaped morphology, which could be rescued by introducing the *CYP77A4* gene. Microscopy revealed that the abnormal patterning was detected at least from the 8-cell stage of the *cyp77a4* embryos. We next analysed auxin distribution in mutant embryos, as the phenotypes resembled those of auxin-related mutants. We found that the auxin response pattern was severely perturbed in the *cyp77a4* embryos owing to an aberrant distribution of the auxin efflux carrier PIN1. CYP77A4 intracellularly localised to the endoplasmic reticulum, which is consistent with the notion that this enzyme acts as an epoxidase of unsaturated fatty acids in the microsomal fraction. We propose that the CYP77A4-dependent metabolic pathway is an essential element for the establishment of polarity in plant embryos.

KEY WORDS: *Arabidopsis thaliana*, Cytochrome P450, Embryonic patterning, Fatty-acid epoxidase, Auxin distribution, Quantitative phenome analysis

INTRODUCTION

Development and metabolism are intertwined with one another during organogenesis. This interaction is essential to maintain the metabolic state in a developmental context-dependent manner. There is also a growing awareness that metabolism plays instructive roles in developmental processes (Bulusu et al., 2017; Carey et al., 2015; Miyazawa et al., 2017; Oginuma et al., 2017; Shang et al., 2016; Toyokura et al., 2011; Tsukagoshi et al., 2010; Sciacovelli et al., 2016). The emerging picture depicts metabolism as a crucial

[1]Okazaki Institute for Integrative Bioscience, 5-1, Higashiyama, Myodaiji, Okazaki, Aichi 444-8787, Japan. [2]National Institute for Basic Biology, 38 Nishigonaka, Myodaiji, Okazaki, Aichi 444-8585, Japan. [3]Department of Basic Biology, School of Life Science, Graduate University for Advanced Studies (SOKENDAI), 38 Nishigonaka, Myodaiji, Okazaki, Aichi 444-8585, Japan. [4]RIKEN Center for Sustainable Resource Science, 1-7-22, Suehiro, Tsurumi, Yokohama, Kanagawa 230-0045, Japan. [5]Department of Biological Sciences, Graduate School of Science, University of Tokyo, 7-3-1 Hongo, Bunkyo-ku, Tokyo 113-0033, Japan.
*Present address: Exploratory Research Center on Life and Living Systems (ExCELLS), 5-1, Higashiyama, Myodaiji, Okazaki, Aichi 444-8787, Japan.
‡These authors contributed equally to this work

§Authors for correspondence (kawa-ken@nibb.ac.jp; masami.hirai@riken.jp)

K.K., 0000-0003-1701-4567; H.K., 0000-0001-7060-9565; H.T., 0000-0002-4430-4538; M.Y.H., 0000-0003-0802-6208

system not only for sustaining physiological conditions, but also for regulating developmental patterning by coordinating various cellular processes (Teleman, 2016).

Forward genetic screenings of *Arabidopsis thaliana* (hereafter, *Arabidopsis*) mutants with developmental defects have led to the discovery of genes encoding metabolic enzymes, which have crucial roles in controlling plant development. Cytochrome P450 proteins are haem-dependent enzymes that catalyse a wide variety of mono-oxygenation and hydroxylation reactions (Mizutani and Ohta, 2010; Schuler and Werck-Reichhart, 2003). The cytochrome P450 genes constitute one of the largest families in the plant genome; for example, they comprise ∼250 genes in *Arabidopsis*. It is widely accepted that the biosynthesis and/or catabolism of phytohormones by cytochrome P450 proteins play pivotal roles in plant development (Mizutani and Ohta, 2010; Nelson and Werck-Reichhart, 2011). In addition, *KLUH/CYP78A5* (also known as *AT1G13710*) has been shown to promote cell proliferation in petals by producing an as-yet-unknown signalling molecule, which is thought to be independent from any classical phytohormone (Anastasiou et al., 2007). The homologous gene most closely related to *KLUH/CYP78A5* is *CYP78A1* (also known as *GRMZM2G167986*), which is expressed preferentially in developing inflorescences of *Zea mays* (Larkin, 1994). Because CYP78A1 has been shown to have a catalytic activity for ω-hydroxylation of lauric acid *in vitro* (Imaishi et al., 2000), the enzymatic function of *KLUH/CYP78A5* is speculated to be fatty acid modification (Anastasiou et al., 2007). Other members of the CYP78A family also contribute to regulating developmental processes, e.g. in seed growth [*CYP78A6* (also known as *AT2G46660*), Fang et al., 2012], fruit morphogenesis [*CYP78A9* (also known as *AT3G61880*), Ito and Meyerowitz, 2000] and determination of the time intervals between leaf initiations (plastochron) [*PLASTOCHRON1/CYP78A11* (also known as *Os10g0403000*), Miyoshi et al., 2004].

In addition to the members of the CYP78 family, CYP77A6 (also known as AT3G10570) also links metabolism to a specific developmental process. This enzyme catalyses in-chain fatty acid hydroxylation to produce cutin polyester. Although the *cyp77a6* mutant lacks the cuticle matrix on the petal surface and the nano-ridge structure beneath the matrix, some electron-dense material, which is a constituent of the nano-ridge structure in the wild type (WT), is detectable (Li-Beisson et al., 2009). This suggests that CYP77A6-mediated metabolism is required for the production of cuticle matrix on the petal surface; thereafter, it helps to form the correct nano-ridge structure. These previous studies indicate that various cytochrome P450 proteins have specific roles in plant development. However, the developmental function of many of these proteins remains unclear (Mizutani and Ohta, 2010). It is thus important to identify the functions of cytochrome P450-encoding genes in developmental regulation through metabolite modification.

DEVELOPMENT

1

This poses a crucial challenge in modern functional genomic studies of cytochrome P450 genes in plant development and metabolism.

Advances in metabolome, transcriptome and proteome analyses, in combination with bioinformatics techniques, allow us to speculate on the metabolic functions of genes (Hirai et al., 2004; Ideker et al., 2001; Keurentjes, 2009; Saito et al., 2008). These approaches facilitate the identification and functional characterisation of genes of interest in metabolism using reverse genetics (Ginglinger et al., 2013; Hirai et al., 2007; Malitsky et al., 2008; Morohashi et al., 2012; Yonekura-Sakakibara et al., 2008). However, developmental traits result from concerted actions across different levels of biological hierarchy, from molecule to tissue and organ, and cannot be fully characterised by molecular-level 'omics' data alone. Because of this limitation, reverse genetics studies focused on the interaction between development and metabolism are limited. Systematic characterisation of developmental phenotypes (the so-called 'phenome') (Kuromori et al., 2006; Toyoda and Wada, 2004; Wilson-Sánchez et al., 2014) in metabolism-related mutants would help to connect metabolic regulation with developmental patterning.

In this study, we analysed cytochrome P450 mutants in *Arabidopsis* and obtained quantitative phenome data to identify a novel mutant that sheds light on the interaction between development and metabolism. We found that the cytochrome P450 mutant *cyp77a4* (*at5g04660*) exhibits a developmental defect in embryonic patterning. By using auxin-related reporters, we showed that *CYP77A4* is involved in shaping the auxin response pattern in embryos by regulating the distribution of an auxin efflux carrier, PIN-

FORMED1 (PIN1) (Benková et al., 2003; Friml et al., 2003; Xu et al., 2006). As CYP77A4 has fatty-acid epoxidation activity in the microsomal fraction (Sauveplane et al., 2009), our study highlights the importance of P450-mediated fatty-acid modification in embryogenesis. More generally, our study indicates that quantitative phenome analysis of metabolism-related mutants is a novel method for functional identification of metabolic genes in plant development.

RESULTS

Functional screening of cytochrome P450 genes based on developmental traits

We first collected 35 *Arabidopsis* T-DNA insertion mutants of cytochrome P450 genes (Table S1) and quantified 12 non-biased developmental traits to identify potential cytochrome P450 genes involved in developmental regulation (Fig. 1A). We validated this approach based on the detection of previously reported smaller rosettes in *cyp79f1* (*at1g16410*) (Reintanz et al., 2001) and shorter petioles in *cyp85a2* (*at3g30180*) (Kim et al., 2005) as positive controls (Fig. 1A). We found that the cotyledon in a *cyp77a4* mutant (*SALK_046395*) was smaller than in the WT, whereas other developmental traits were largely comparable with the WT (Fig. 1A). This obvious reduction in size was unique among the 35 mutants. A public microarray database (eFP-browser, bar.utoronto. ca/efp/cgi-bin/efpWeb.cgi) indicated that *CYP77A4* is expressed primarily in early-stage embryos (Winter et al., 2007; Fig. S1), suggesting that it is involved in embryogenesis. The enzymatic function of CYP77A4 is proposed to be as an epoxidase of
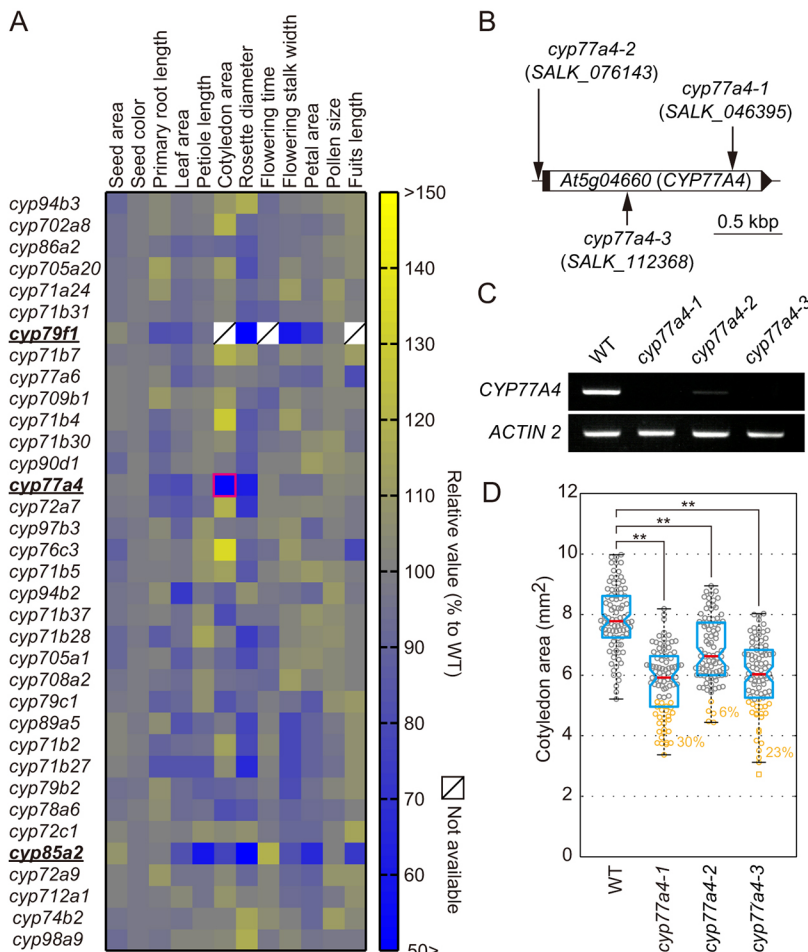

Fig. 1. Smaller cotyledon phenotype in *cyp77a4* identified from phenome data. (A) Twelve developmental traits were measured in 35 cytochrome P450 mutants. Colour intensity from yellow (positive) to blue (negative) indicates the relative value of each trait compared with the WT. Cotyledon area in the *cyp77a4* mutant (*SALK_046395*) is marked by a magenta square. Owing to severe growth defects, data on cotyledon area, rosette diameter and fruit length could not be determined in the *cyp79f1* mutant. (B) Schematic of the *CYP77A4* gene and the position of the T-DNA insertions. Exon is shown as an open rectangle; 5′- and 3′-untranslated regions are shown as a filled rectangle and triangle, respectively; non-transcribed flanking regions are shown as horizontal lines. There is no intron in this gene. (C) Semi-quantitative RT-PCR analysis of *CYP77A4* expression in the immature seeds of the WT and three *cyp77a4* mutant alleles. *ACTIN 2* was used as an internal control. (D) Cotyledon area in the WT and three T-DNA insertional *cyp77a4* mutants. The box indicates the interquartile range and the horizontal red line represents the median. A notch approximates a 95% confidence interval for the median. **$P < 0.01$ compared with WT (Mann–Whitney U-test). The line outside the box represents the maximum to minimum values without outliers. An outlying value greater than 50% is indicated by a square. The smaller sized population in the mutants compared with WT population is marked in orange. $n = 90$.
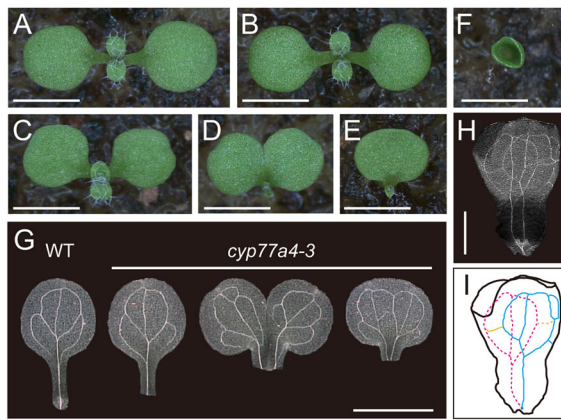
Fig. 2. Irregular arrangement of cotyledons in the *cyp77a4* mutants. (A-F) Cotyledons of 7-day-old seedlings in the WT (A) and the *cyp77a4-3* mutant (B-F). WT-like (B), abnormally arranged (C), single (D,E) and cup-shaped (F) cotyledons in the *cyp77a4-3* mutant are shown. (G-I) Vascular pattern of cotyledons in the WT and the *cyp77a4-3* mutants (G). The cup-shaped cotyledon corresponding to F was also cleared (H) and visualised vasculature is depicted in I. The blue solid line and magenta dotted line indicate vasculatures on the front and back sides, respectively. Orange lines indicate veins connecting these vasculatures. Scale bars: 2 mm.

unsaturated fatty acids, including linoleic acid, to produce vernolic acid, which is a precursor of antifungal compounds (Hou and Forman, 2000; Pinot and Beisson, 2011; Sauveplane et al., 2009). However, the developmental role of CYP77A4 is still unclear. We therefore selected *CYP77A4* for further functional investigation.

Irregular arrangement of cotyledons in the *cyp77a4* mutant

We confirmed that the *SALK_046395* allele contains a T-DNA insertion in the exon of the *AT5G04660* locus (Fig. 1B). T-DNA insertions in the 82 bp upstream region and in the exon were also verified in two independent available alleles (*SALK_076143* and *SALK_112368*, respectively) (Fig. 1B). These three alleles are hereafter referred to as *cyp77a4-1* (*SALK_046395*), *cyp77a4-2* (*SALK_076143*) and *cyp77a4-3* (*SALK_112368*). The *CYP77A4* transcript was undetectable in the *cyp77a4-1* and *cyp77a4-3* alleles, and present at a low level in the *cyp77a4-2* allele (Fig. 1C). All three alleles exhibited the smaller cotyledon phenotype compared with the WT with 30%, 6% or 23% penetrance in *cyp77a4-1*, *cyp77a4-2* or *cyp77a4-3*, respectively (Fig. 1D). We detected a significant decrease in cell number, but not in cell area, in the null alleles *cyp77a4-1* and *cyp77a4-3* (Fig. S2). This indicated that a cell proliferation defect is a primary cause for the decrease in cotyledon size in the mutants.

In addition to the abnormality in size, we found that cotyledon arrangement was perturbed in the *cyp77a4* mutants. Whereas

bilateral arrangement of cotyledons was present in the WT and was predominant among *cyp77a4* mutants (Fig. 2A,B; Table 1), irregular arrangement of cotyledons was also observed among mutants (Fig. 2C; Table 1). More-severe defects in the cotyledon phenotype of the *cyp77a4* mutants included single or cup-shaped cotyledons (Fig. 2D-F; Table 1). A single central mid-vein with some lateral veins was formed in the morphologically normal cotyledons of the WT and the *cyp77a4* mutants (Fig. 2G). We observed two sets of this vascular pattern within the single or cup-shaped mutant cotyledons (Fig. 2G-I). This suggested that bilateral symmetry is, at least partially, maintained within an individual mutant despite the severe cotyledon phenotype. These phenotypes could be rescued by introducing the genomic fragment containing *AT5G04660*, from 1.58 kb upstream of the initiation codon to its stop codon, into the *cyp77a4-3* mutant (*cyp77a4-3/pCYP77A4::CYP77A4*) (Table 2), showing that *CYP77A4* is responsible for the developmental defect in cotyledons.

cyp77a4 exhibits defects in embryonic patterning from early developmental stages

Our complementation test using the *cyp77a4-3/pCYP77A4::CYP77A4* transgenic lines showed that the upstream 1.58 kb fragment was sufficient to induce the expression of *CYP77A4* for proper cotyledon patterning. We established β-glucuronidase (GUS)-reporter lines using the fragment as a *CYP77A4* promoter (*pCYP77A4::GUS*) to investigate the expression profile of *CYP77A4*. GUS staining was observed in the embryos, but was undetectable in other tissues in immature seeds from 5-week-old plants (Fig. 3A-C). We confirmed the accumulation of *CYP77A4* transcripts in embryos by whole-mount *in situ* hybridisation (Fig. S3). *CYP77A4* promoter activity seemed to be absent after germination, except in trichomes (Fig. 3D-H). Quantitative real-time reverse-transcription PCR (qRT-PCR) yielded results consistent with those of the expression analyses (Fig. 3I), indicating that *CYP77A4* is expressed primarily in embryos.

Given the expression pattern of *CYP77A4*, we observed the *cyp77a4* embryos to characterise developmental defects during embryogenesis. We found that the mutants exhibited irregular cell division, resulting in uncoordinated tissue patterning from early embryogenesis (Fig. 4A,E; Figs S4-S5). Similar defects were observed in subsequent developmental stages in the mutants, as evidenced by the lack of characteristic globular and heart shapes for

Table 1. Frequencies of cotyledon phenotypes in three *cyp77a4* alleles

Genotype	One	Two (irregular)	Two (normal)	Three	Total number
WT	0	0	100.0	0	964
cyp77a4-1	0.9	0.8	98.2	0	962
cyp77a4-2	0.2	0.1	99.7	0	1018
cyp77a4-3	1.5	0.2	98.3	0	1273

The unseparated cotyledon (Fig. 2D) and cup-shaped cotyledon (Fig. 2F) were counted as 'One', in addition to the single cotyledon (Fig. 2E). Two separated cotyledons with bilateral asymmetry around the shoot apical meristem (Fig. 2C) were counted as 'Two (irregular)'.

Table 2. Frequencies of cotyledon phenotypes in the transgenic lines

Genotype	One	Two (irregular)	Two (normal)	Three	Total number
WT	0	0	100.0	0	965
cyp77a4-3	0.9	0.6	98.4	0	955
cyp77a4-3/ pCYP77A4:: CYP77A4	0	0	100.0	0	966
cyp77a4-3/ pCYP77A4:: CYP77A4-GFP	0	0	100.0	0	991
cyp77a4-3/ pCYP77A4:: GFP	1.4	1.0	97.6	0	1047

The unseparated cotyledon (Fig. 2D) and cup-shaped cotyledon (Fig. 2F) were counted as 'One', in addition to the single cotyledon (Fig. 2E). Two separated cotyledons with bilateral asymmetry around the shoot apical meristem (Fig. 2C) were counted as 'Two (irregular)'.
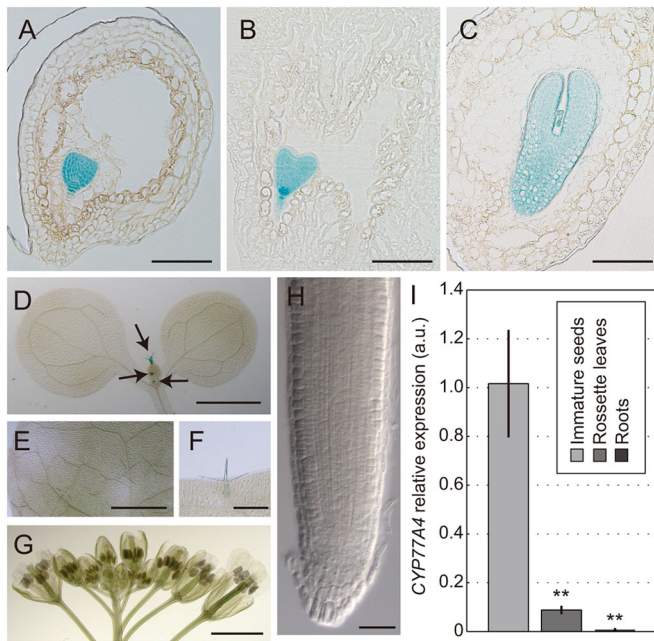
Fig. 3. Tissue-specific activity of the *CYP77A4* promoter. (A-H) GUS-stained immature seed sections (A-C), cotyledons and young leaf primordia (D), fully-expanded leaf (E), mature trichome (F), flower buds (G) and root (H) of *pCYP77A4::GUS*. Scale bars: 100 μm in A-C; 1 mm in D,E; 200 μm in F; 2 mm in G; 50 μm in H. Arrows indicate developing trichomes. (I) Expression levels of *CYP77A4* in immature seeds 80 h after flowering, rosette leaves and roots of the WT. Transcription levels were normalised with that of *UBC9* (WT=1.0). Data are mean±s.d. (*n*=3 for biological replicates, with analytical triplicate in each sample). **P*<0.01 compared with the WT (Student's *t*-test).
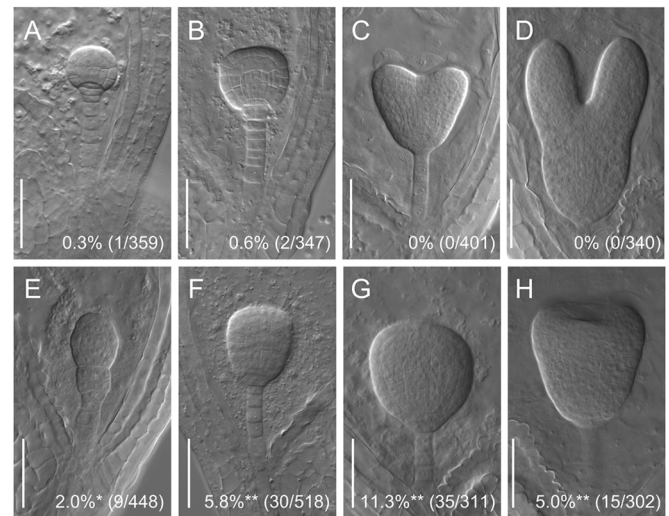

Fig. 4. *CYP77A4* is required for embryonic patterning. (A-H) Differential interference contrast (DIC) images of cleared immature seeds. Embryos at earlier-than-globular, globular, heart and torpedo developmental stages in the WT (A-D) and at the corresponding stages in the *cyp77a4-3* mutants (E-H). Representative pictures of embryos with severe defects are shown. Penetrance of the mis-shaped embryo in the mutants was calculated as a frequency of the number of abnormal embryos against the total number observed. **P*<0.05, ***P*<0.01 compared with WT (two-tailed Fisher's exact test). Developmental stages in the mutant were estimated based on the morphology of other normal embryos from the same fruit. Samples were collected from 5-week-old plants. Scale bars: 50 μm.

embryos (Fig. 4B,C,F,G; Fig. S5). Whereas two cotyledon primordia were separately grown at the torpedo stage in the WT, the boundary between cotyledon primordia was obscure at the comparable stage in the mutant (Fig. 4D,H; Fig. S5). The penetrance of the mis-shaped embryo at the torpedo stage is relatively milder than that at the heart stage (Fig. 4G,H; Fig. S5), suggesting that morphological defects might be, at least partially, fixed toward the torpedo and/or later developmental stages.

These results strongly suggested that the irregular arrangement of cotyledons, and single or cup-shaped cotyledon morphology, are formed by a failure of embryonic patterning, owing to the absence of the separation boundary between cotyledon primordia, rather than by the fusion of two emerging primordia. In contrast to mutant embryos, we detected no morphological defect in mutant trichomes (Fig. S6).

Establishment of auxin response maximum is impaired in the *cyp77a4* mutants

Cotyledon development in embryonic patterning requires the auxin response maximum at cotyledon primordia (Aida et al., 2002; Benková et al., 2003; Friml et al., 2003; Furutani et al., 2004; Treml et al., 2005). Morphological defects in the *cyp77a4* embryos suggested an abnormal pattern of auxin response. To examine this possibility, we crossed a transgenic line expressing a gene that encodes GREEN FLUORESCENT PROTEIN (GFP) driven by the auxin-responsive promoter *DR5_{rev}* (*DR5_{rev}::GFP*; Friml et al., 2003) with the *cyp77a4-3* mutant (*cyp77a4-3/DR5_{rev}::GFP*) and performed confocal microscopy. Local auxin response, as represented by GFP fluorescence, was observed in the hypophysis at first (100%, *n*=288), and gradually became evident in the tips of

emerging cotyledon primordia against the WT background (100%, *n*=312) (Fig. 5A-I). In contrast, the GFP fluorescence was often absent in the entirety of the early embryo (11.5%, *n*=364) (Fig. 5J-L), or it was expanded with very weak intensity or undetectable in the apical domain of the embryos without a clear separation boundary between cotyledon primordia against the *cyp77a4-3* background (13.3%, *n*=339) (Fig. 5M-R). These penetrances in the *cyp77a4-3* mutants were significantly higher than in the WT (*P*<0.01, two-tailed Fisher's exact test). The pattern of *DR5_{rev}::GFP* expression was not perturbed in the *cyp77a4-3* roots (Fig. S7), which is consistent with the finding that *CYP77A4* expression was hardly detectable in this tissue, except for during the embryonic stage (Fig. 3A-C,I; Fig. S3).

During embryogenesis, the establishment of an auxin response maximum is facilitated by the characteristic distribution of the PIN1 efflux carrier, which transports auxin downward to the root pole through vascular tissue and upward to the tips of emerging cotyledon primordia through protodermal tissue (Benková et al., 2003; Friml et al., 2003). We next investigated whether the inappropriate distribution of an auxin response maximum in the *cyp77a4* embryos was due to a defect in the PIN1 expression pattern. PIN1 localisation was visualised using transgenic lines that express a gene that encodes PIN1 fused with ENHANCED GFP (EGFP) driven by the *PIN1* promoter against the WT background (*pPIN1::PIN1-EGFP*, Xu et al., 2006) and the *cyp77a4-3* background (*cyp77a4-3/pPIN1::PIN1-EGFP*). The overall distribution of PIN1-EGFP was largely similar between the WT and the *cyp77a4-3* mutant embryos with relatively normal shape (Fig. 6A-C,E-G,I-K). However, at a cellular level we found that PIN1-EGFP fluorescence was often absent in the tips of cotyledon primordia in the *cyp77a4-3* embryos, in contrast to the WT (Fig. 6D,H). Although protodermal cell division is predominantly anticlinal to
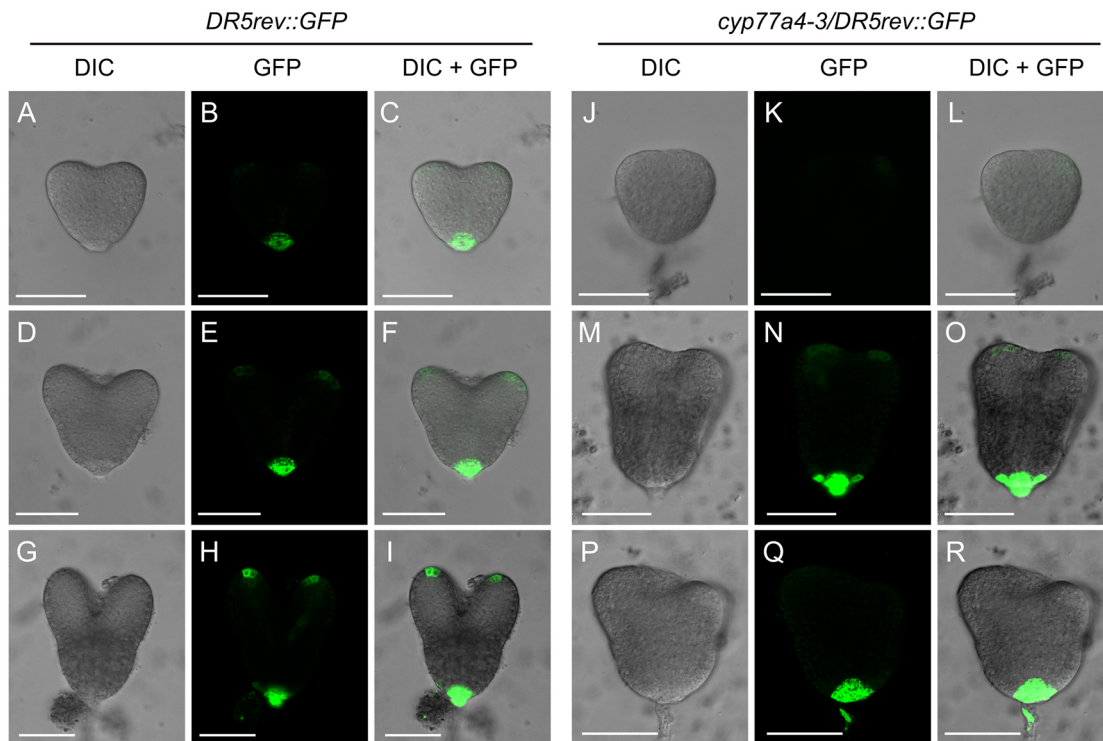
Fig. 5. Expression of *DR5$_{rev}$::GFP* in WT and *cyp77a4* embryos. (A-I) DIC (A,D,G), GFP fluorescence (B,E,H) and merged (C,F,I) images of triangular (A-C), early heart (D-F) and late heart (G-I) stages of *DR5$_{rev}$::GFP* embryos. (J-R) DIC (J,M,P), GFP fluorescence (K,N,Q) and merged images (L,O,R) of *cyp77a4-3/DR5$_{rev}$::GFP* embryos. Embryos without cotyledon primordia protrusions (J-L) and without clear separation boundaries between cotyledon primordia (M-R) are shown. Scale bars: 50 µm.

the surface of embryos in the WT for correct auxin distribution, we observed the periclinal or oblique division plane in the *cyp77a4-3* embryos, in which PIN1-EGFP was accumulated (Fig. 6L; Fig. S4). In the *cyp77a4-3* embryo without protrusions of cotyledon primordia, PIN1-EGFP fluorescence was very weak and its localisation was often missing in the tip of cotyledon primordia (Fig. 6P). These results suggested that CYP77A4 is involved in the correct distribution of PIN1, and thus proper shaping of an auxin response maximum for a coordinated cell-division pattern during embryogenesis.

CYP77A4 localises to the endoplasmic reticulum membrane
The epoxide derivative of linoleic acid (vernolic acid) is produced by CYP77A4 and is subsequently metabolised by epoxide hydrolases in *Arabidopsis* microsomes (Sauveplane et al., 2009). To examine whether subcellular localisation of CYP77A4 is spatially consistent with this metabolic pathway, we transiently expressed *CYP77A4-GFP* or *GFP-CYP77A4* in mesophyll protoplast cells using the cauliflower mosaic virus *35S* promoter. We prepared protoplasts from WT as a negative control of background fluorescence (Fig. 7A,B) or from a transgenic line that expresses monomeric RED FLUORESCENCE PROTEIN (mRFP) fused with the functional soluble *N*-ethylmaleimide sensitive factor attachment protein receptor (SNARE) VAM3/ SYP22 (AT5G46860) (mRFP-VAM3) to visualise vacuole-related membranes (Ebine et al., 2008) (Fig. 7C,D). In contrast to the GFP (Fig. 7E,F), CYP77A4-GFP fluorescence was observed in the cell periphery, transvacuolar cytoplasmic strands and perinuclear region, which overlapped with mRFP-VAM3 fluorescence (Fig. 7G-R). We detected no GFP-CYP77A4 fluorescence, likely because *N*-terminal GFP fusion may perturb CYP77A4 localisation

by preventing its *N*-terminal hydrophobic domain from anchoring to the membrane (Fig. 7S,T). We then established *cyp77a4-3* transgenic lines expressing *CYP77A4-GFP* using the *CYP77A4* promoter (*cyp77a4-3/pCYP77A4::CYP77A4-GFP*) to confirm the intracellular localisation of CYP77A4. The mutant phenotype in cotyledon patterning was fully rescued by the expression of CYP77A4-GFP (Table 2), indicating its functionality. Confocal microscopy showed that CYP77A4-GFP fluorescence was most evident in the protodermal cell layer of the embryos (Fig. 7U). Intracellularly, we detected CYP77A4-GFP fluorescence around the nucleus, cell periphery and cytoplasmic strands, similar to our transient assay with protoplasts (Fig. 7V,W), in contrast to the negative control of GFP fluorescence (Fig. 7X). Based on these observations, we concluded that CYP77A4 localises to the endoplasmic reticulum membrane.

Double mutant analysis using *cyp77a4* and *cyp77a6*
CYP77A6 is the gene exhibiting the closest homology to *CYP77A4*, and it regulates fatty acid modification in floral organs (Li-Beisson et al., 2009). To examine whether *CYP77A6* is also involved in cotyledon development during embryogenesis, we observed the cotyledon phenotype in the *cyp77a6* mutants. We determined that these mutants produced normal cotyledons (Table S2). The frequency of the cotyledon phenotype in the *cyp77a4-3 cyp77a6-2* double mutant is similar to that in the *cyp77a4-3* (Table S3). Overall, the growth of the double mutant was comparable with that of the WT in mature plants (Fig. S8). These data indicate that the developmental function of CYP77A4 is independent of CYP77A6.

The *cyp77a6* petal is readily stained with Toluidine Blue, owing to the lack of cuticle matrix on the petal surface (Li-Beisson et al., 2009). We tested whether dye permeability was affected by the
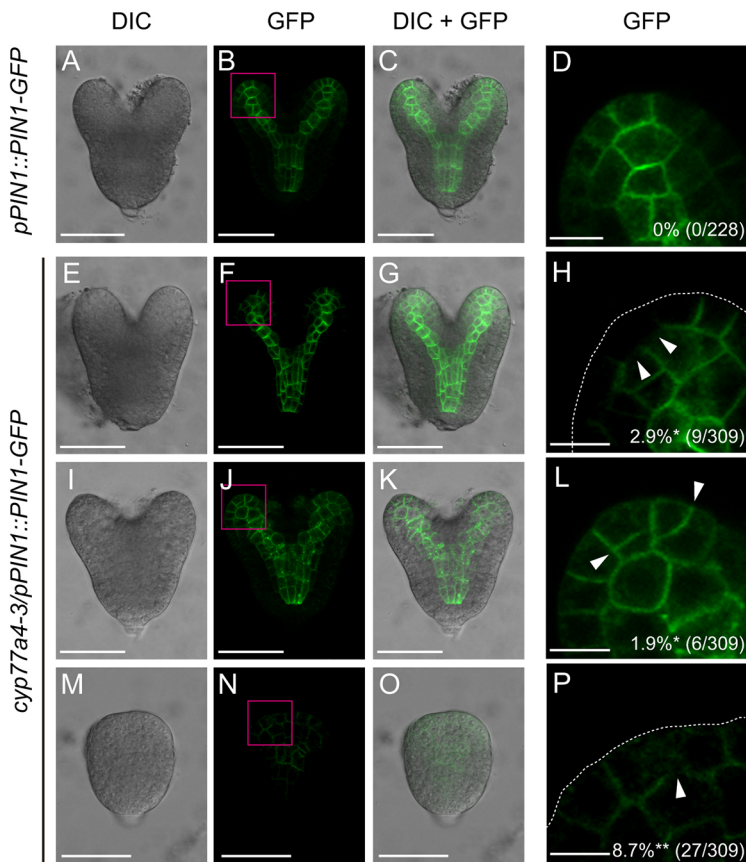
Fig. 6. Distribution of PIN1-GFP in WT and *cyp77a4* embryos. (A-D) DIC (A), PIN1-GFP fluorescence (B) and merged image (C) of the *pPIN1::PIN1-GFP* embryo. The boxed area in B is magnified in D. (E-P) DIC (E,I,M), PIN1-GFP fluorescence (F,J,N) and merged images (G,K,O) of the *cyp77a4-3/pPIN1::PIN1-GFP* embryos. The boxed areas in F,J,N are magnified in H,L,P, respectively. Arrowheads indicate aberrant PIN1-GFP missing (H,P) or localisation (L) sites. Scale bars: 50 μm in A-C,E-G,I-K,M-O; 10 μm in D,H,L,P. Penetrance of the aberrant PIN1-GFP expression was calculated as a frequency of the number of embryos showing the aberrant PIN1-GFP expression against the total number observed. *$P<0.05$ and **$P<0.01$ compared with WT (two-tailed Fisher's exact test).

cyp77a4 mutation, to further investigate the functional relationship between *CYP77A4* and *CYP77A6*. In contrast to the petals on the *cyp77a6-2* mutant, petals on the *cyp77a4-3* mutant were not permeable to dye, similar to the WT (Fig. S9A-C). Petals on the *cyp77a4-3 cyp77a6-2* double mutant showed similar dye permeability to *cyp77a6-2* petals (Fig. S9C,D). Although *CYP77A4* is expressed in trichomes (Fig. 3D,F), the dye did not permeate into the trichomes of the *cyp77a4-3* mutant, similar to results seen in the WT (Fig. S9E,F,I,J). This impermeability was also observed in the trichomes of *cyp77a6-2* and the *cyp77a4-3 cyp77a6-2* double mutant (Fig. S9E-L). Interestingly, dye permeability slightly increased in the germinating embryos of *cyp77a4-3* and *cyp77a4-3 cyp77a6-2* double mutant, compared with WT and *cyp77a6-2* (Fig. S9M-P). These data suggest that CYP77A4 is involved in the production of cuticle matrix, but it is limited within embryos and can be spatially separable from the CYP77A6 function in petals.

DISCUSSION
We performed quantitative phenome screening of cytochrome P450 mutants to identify a novel metabolic gene involved in plant development. This analysis revealed that CYP77A4, which is able to catalyse the fatty-acid epoxidation (Sauveplane et al., 2009), participates in cotyledon development during embryogenesis. We showed that CYP77A4 facilitates proper PIN1 distribution within embryos, thereby promoting the establishment of an auxin response maximum for polarity formation and organised cell-division patterning. Although auxin action in embryos is well established (Aida et al., 2002; Benková et al., 2003; Friml et al., 2003; Furutani et al., 2004; Treml et al., 2005), our study provides new molecular insight into this process. Interestingly, we found that CYP77A4 has

specific developmental functions in this embryonic process, indicating that the CYP77A4-dependent metabolite modification is involved in polarity establishment in a developmental context-dependent manner. In addition, our study shows that quantitative phenome screening could determine as-yet-unknown developmental functions of the cytochrome P450 genes. Given that transcriptome and metabolome techniques are widely applied to elucidate the molecular function of metabolism-related genes (Ehlting et al., 2008; Ginglinger et al., 2013; Hirai et al., 2004, 2007), we propose that quantitative phenome-based analysis further links molecular function with developmental control.

CYP77A4-dependent regulation of auxin distribution in embryos
Several lines of evidence indicate that lipid modification is a major requirement for correct auxin distribution, facilitated by polar positioning of auxin efflux carriers, including PIN1. *STEROL METHYLTRANSFERASE1* (*SMT1*, also known as *AT5G13710*) is involved in sterol biosynthesis through methylation (Diener et al., 2000; Schrick et al., 2002). Various defects are observed in the embryo, vasculature and root patterning of the *smt1* mutants, owing to aberrant cell polarity caused by PIN1 mislocalisation. Because the level of a major membrane sterol, sitosterol, is decreased in the *smt1* mutant, it has been suggested that a sterol-dependent microdomain (or lipid raft) contributes to the polarised PIN1 localisation (Willemsen et al., 2003). An alternative explanation is that PIN1 transportation is associated with sterol-dependent polar trafficking (Grebe et al., 2003). A recent study focusing on other types of sterol methyltransferases [SMT2 (AT1G20330) and SMT3 (AT1G76090)] showed that sterol modification by these enzymes is involved in the endocytic recycling required for PIN2 polar
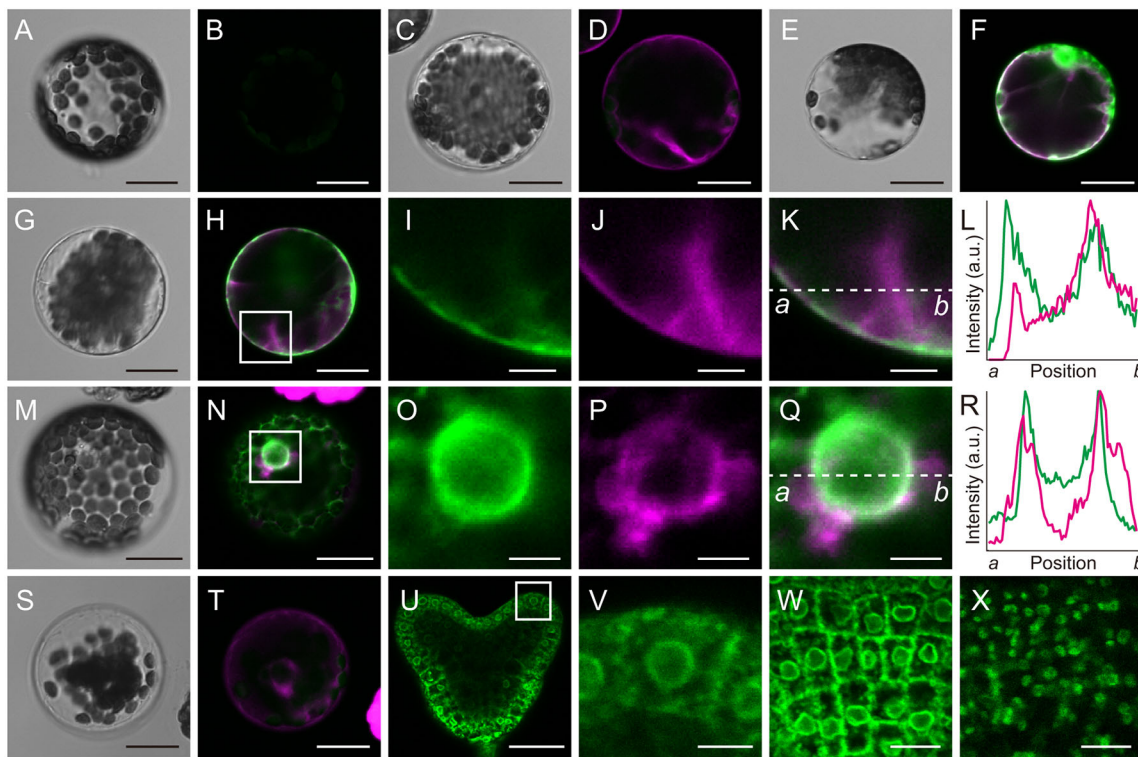
Fig. 7. Subcellular localisation of CYP77A4 on endoplasmic reticulum. (A-T) Untransfected WT mesophyll protoplasts (A,B), untransfected *vam3-1/pVAM3::mRFP-VAM3* mesophyll protoplasts (C,D), *35S::GFP*-transfected *vam3-1/pVAM3::mRFP-VAM3* mesophyll protoplasts (E,F), *35S::CYP77A4-GFP*-transfected *vam3-1/pVAM3::mRFP-VAM3* mesophyll protoplasts (G-K,M-Q) and *35S::GFP-CYP77A4*-transfected *vam3-1/pVAM3::mRFP-VAM3* mesophyll protoplasts (S,T). DIC images (A,C,E,G,M,S) and merged images of GFP and mRFP channels (B,D,F,H,N,T) are shown. Magnified view of the boxed areas in H and N are indicated in I-K and O-Q, respectively. GFP (I,O), mRFP (J,P) and merged images (K,Q) are shown. Normalised intensity profiles of GFP (green) and mRFP (magenta) between *a* and *b* in K and Q are plotted in L and R, respectively. (U,V) Fluorescence images of the embryo in *cyp77a4-3/pCYP77A4::CYP77A4-GFP*. Magnified view of the boxed area in U is shown in V. (W,X) Fluorescence images of protodermal cells of the embryos in *cyp77a4-3/pCYP77A4::CYP77A4-GFP* (W) and *cyp77a4-3/pCYP77A4::GFP* (X) as a control. Scale bars: 20 µm in A-H,M,N,S,T; 5 µm in I-K,O-Q,V; 30 µm in U; 10 µm in W,X.

localisation in roots (Nakamoto et al., 2015). Similar pleiotropic defects in development were also observed in mutants of the fatty-acid biosynthesis pasticcino genes (Baud et al., 2004; Bellec et al., 2002; Haberer et al., 2002; Kajiwara et al., 2004; Roudier et al., 2010). Our observed phenotype in the *cyp77a4* mutants may be attributable to missing or perturbed PIN1 polar localisation, and the resultant aberrant distribution of auxin, in the embryos. Therefore, based on these results, in combination with the proposed enzymatic function of CYP77A4 in fatty-acid epoxidation (Sauveplane et al., 2009), we assume that the molecular mechanism by which CYP77A4 contributes to embryonic patterning is related to membrane docking and/or trafficking of PIN1 for its polar localisation by adjusting fatty-acid composition. Besides auxin transport, local auxin production is also important for embryonic patterning (Robert et al., 2013; Stepanova et al., 2008). It would be informative to test whether auxin biosynthesis is affected or not in the *cyp77a4* mutant embryos.

It appears that the CYP77A4-mediated formation of an auxin response maximum is absent in other tissues, such as roots, as our phenome analysis detected little difference in developmental traits other than cotyledon size in the *cyp77a4* mutant. This is consistent with the expression pattern of *CYP77A4* in only embryos and trichomes, and normal *DR5rev::GFP* expression in roots. One attractive hypothesis is that the optimal lipid composition for polarity establishment differs between tissues. However, we cannot exclude the possibility that other enzymes can compensate for the deficit of CYP77A4 in other tissues.

CYP77A6 is phylogenetically close to *CYP77A4* among CYP77 family members (Li-Beisson et al., 2009). Whereas *CYP77A4* is expressed in the embryos to establish auxin distribution, CYP77A6 action for cutin polyester biosynthesis is limited to the petal surface (Li-Beisson et al., 2009). The *cyp77a4 cyp77a6* double mutant does not exhibit ubiquitous growth defects, as are observed in biosynthesis mutants of sterols or very-long-chain fatty acids (Kajiwara et al., 2004; Nakamoto et al., 2015; Roudier et al., 2010; Willemsen et al., 2003). These data suggest that the auxin-related developmental function of CYP77A4 is independent of CYP77A6. Identifying and characterising other epoxidases in *Arabidopsis* will facilitate further investigation of this issue.

Role of epoxidation in plant development
CYP77A4 is the first cytochrome P450 that has been reported as being able to catalyse the epoxidation of fatty acids in *Arabidopsis* (Sauveplane et al., 2009). A previous study demonstrated that vernolic acid is converted to the corresponding diol in the *Arabidopsis* microsomal fraction. Because the resulting diol has antifungal properties (Hou and Forman, 2000), the function of CYP77A4 is speculated to be as a defence response (Pinot and Beisson, 2011; Sauveplane et al., 2009). Our GUS-reporter assay using the *CYP77A4* promoter showed that the promoter is active in trichomes, as well as in embryos. A publicly available database of genes expressed in trichomes (TrichOME, www.planttrichome.org/) (Dai et al., 2010) also indicated that the *CYP77A4* transcript is detectable in *Arabidopsis* trichomes. Based on this expression

pattern, the synthesis of a defensive compound by CYP77A4 through the vernolic acid pathway appears to be viable in trichomes. In addition to this function, we propose that the CYP77A4-dependent metabolic pathway is related to embryonic patterning. Given that CYP77A4 widely catalyses the epoxidation of unsaturated fatty acids, including linoleic acid (Sauveplane et al., 2009), this enzyme can affect metabolic pathways during embryogenesis other than those that are linoleic acid related. We indeed detected that *CYP77A4* knockout or overexpression has little effect on linoleic acid content in immature seeds compared with the WT, as well as on compounds chiefly related to central carbon metabolism and amino acids (Y.L., Y.S., M.O. and M.Y.H., unpublished). We found that CYP77A4 also participates in cuticle matrix production in embryos, based on the Toluidine Blue permeability test. This might be the key to identifying relevant substrates of CYP77A4 that are required for auxin-mediated embryonic patterning.

Whereas epoxidation of fatty acids in animals is well studied because of the biological activities of derivatives (Catella et al., 1990; Roman, 2002; Zeldin et al., 1996), less attention has been paid to P450-mediated epoxidation in plants. We shed light on this topic by uncovering the function of CYP77A4 in plant development. This finding could extend understanding of the P450-mediated metabolic regulation of development by linking epoxidation to the establishment of polarity. Future work to analyse the comprehensive lipid composition within embryos, focused in particular on epoxidation, with solid biochemical evidence for CYP77A4 enzymatic activity, and any links to the developmental function will uncover how this modification affects the metabolic regulation of plant development.

MATERIALS AND METHODS
Plant materials and growth conditions
The *Arabidopsis* WT accession used in this study was Colombia-0. Cytochrome P450 T-DNA insertion mutants were included in an allele set of confirmed T-DNA insertion lines (CS27941) provided by the *Arabidopsis* Biological Resource Center. Homozygous mutation was confirmed by genotyping PCR using primers that are listed in Tables S1 and S4. Before analysis, all *cyp77a4* alleles were backcrossed with the WT three times. The *cyp77a4-1* or *cyp77a4-3* mutation was introduced into the $DR5_{rev}::GFP$ (Friml et al., 2003) and *pPIN1::PIN1-EGFP* (Xu et al., 2006) transgenic lines by crossing. The *cyp77a6-1* and *cyp77a6-2* mutations were introduced into *cyp77a4-1* and *cyp77a4-3*, respectively, by crossing. Each genotype was confirmed by genotyping PCR using primers that are listed in Table S4. As essentially the same results were obtained irrespective of the *cyp77a4* allelic background, we show representative results against the *cyp77a4-3* background. Plants were grown on rockwool, as has been previously described (Kawade et al., 2010).

Phenome analysis
Dry seeds were observed using a stereoscopic microscope (M165FC; Leica Microsystems) and analysed in terms of size (Herridge et al., 2011) or colour (binary intensity) (*n*>25). Image processing was performed using ImageJ software (imagej.nih.gov/ij/). Primary root length was measured in 7-day-old seedlings that were grown on vertically placed plates (*n*=12). *In vitro* culture was conducted according to a previous study (Kawade et al., 2013). The first leaves from 3-week-old plants were fixed, cleared and observed (Kawade et al., 2013; Tsuge et al., 1996) for measurement of blade area and petiole length (*n*=8). Cotyledon area in 3-week-old plants (*n*=16), and flowering stalk width (*n*=9), pollen size (*n*>14) and fruit length (*n*=27) in 5-week-old plants were measured using a stereoscopic microscope. Rosette diameter was calculated as the average of the longest three leaves in 3-week-old plants (*n*=8). Flowering time was evaluated as has been described elsewhere (*n*=9) (Notaguchi et al., 2008). Petals were collected

from fully opened flowers in 4-week-old plants and observed under the stereoscopic microscope (*n*=9).

Vector construction and establishment of transgenic lines
Because *CYP77A4* does not contain introns, genomic DNA that had been extracted from WT seedlings was used as the template for vector construction. The primers that were used are listed in Table S4. To create the GUS-reporter construct, a 1580 bp region extending from the first intron of the upstream gene (*AT5G04650*) to the 5′-UTR of *CYP77A4* was selected as the promoter construct. The promoter was amplified using primer pair 17 and 19 (Table S4) and introduced into pGWB3 using the TOPO and Gateway system (Invitrogen). To create the overexpression construct, a 1539 bp region spanning the coding region of *CYP77A4* was amplified using primer pair 18 and 20 and introduced into pGWB2. To create complementation and GFP constructs driven by the *CYP77A4* promoter, a 3119 bp region spanning the promoter, 5′-UTR and coding region of *CYP77A4* was amplified using primer pair 17 and 20, and introduced into pGWB1 and pGWB4. For GFP constructs driven by the cauliflower mosaic virus *35S* promoter, the coding region of *CYP77A4* was amplified using primer pairs 18 and 20, or 18 and 21, and introduced into pGWB6 and pGWB5 for the N- and C-terminal GFP fusion constructs, respectively. The pGWB binary vectors are described elsewhere (Nakagawa et al., 2007). These vectors were transformed into the GV3101 *Agrobacterium* strain and introduced into *Arabidopsis* plants. For the GUS-reporter, overexpression and *35S* promoter GFP constructs, the WT was used as a transgenic background. For complementation and own promoter GFP constructs, *cyp77a4-3* was used as the transgenic background. Transgenic lines were screened on agar-solidified 1/2 Murashige and Skoog medium with 25 mg/l hygromycin. T3 homozygous lines were subjected to further experiments.

RT-PCR analysis
Immature seeds were harvested from fruits 80 h after flowering. Shoot and root samples were collected from 3-week-old plants. Total RNA was extracted using the RNeasy Plant Mini Kit (Qiagen) and treated with the DNase TURBO DNA-free kit (Thermo Fisher Scientific) according to the manufacturer's instructions. The first-strand cDNA was synthesised using SuperScript II (Invitrogen) with identical RNA concentration for each sample.

The expression levels of *CYP77A4* in immature seeds of the WT and three *cyp77a4* mutant alleles were analysed using semi-quantitative reverse transcription PCR (RT-PCR). *ACTIN2* (*AT3G18780*) was used as an internal control (Han and Kim, 2006). The expression levels of *CYP77A4* in different tissues was analysed by quantitative real-time reverse-transcription PCR (qRT-PCR). PCR amplification using Fast SYBR Green (Thermo Fisher Scientific) was monitored on the StepOnePlus real-time PCR system (Applied Biosystems). *UBIQUITIN CONJUGATING ENZYME 9* (*UBC9*, also known as *AT4G27960*) was used as an internal control (Hirai et al., 2007). The primers that were used are listed in Table S4. Data were collected from three independent biological replicates with triplicates in each sample, and were subjected to statistical analysis, as described in the figure legends.

Microscopy
Cotyledons from 7-day-old seedlings were fixed in formalin/acetic acid/alcohol solution (FAA) and cleared in chloral hydrate solution (200 g chloral hydrate, 20 g glycerol, 50 ml water) (Tsuge et al., 1996) to observe the vascular pattern with the stereoscopic microscope. Isolated immature seeds from 5-week-old plants were cleared using chloral hydrate solution for observation of embryos with a Nomarski differential interference contrast microscope (DM2500; Leica Microsystems).

Fluorescence microscopy was performed using a confocal laser-scanning microscope (A1Rsi; Nikon). For staining with propidium iodide, root tissue was soaked in 1 mg/ml propidium iodide solution for 1 min, washed several times with water and then observed. Images were processed using NIS-Elements (Nikon), in addition to ImageJ software.

GUS histochemistry
Tissue samples were infiltrated with a reaction buffer [100 mM NaPO$_4$, pH 7.0, 1.5 mM 5-bromo-4-chloro-3-indolyl-β-glucuronic acid, 4.5 mM

8

K$_3$Fe(CN)$_6$, 4.5 mM K$_4$Fe(CN)$_6$, 10 mM EDTA, 0.1% Triton X-100], incubated overnight at 22°C or 37°C and fixed with FAA. Immature seed samples from 5-week-old plants were dehydrated in an ethanol series and embedded in Technovit 7100 (Heraeus). The resin block was sectioned at 5 μm with a rotary microtome (Leica Biosystems) and placed on glass slides for microscopy. We observed three independent *pCYP77A4::GUS* lines and obtained consistent results.

Toluidine Blue staining

The first leaves from 2-week-old plants and flowers from 5-week-old plants were soaked in Toluidine Blue solution with 0.01% Silwet L-77 for 30 min, then washed several times with water before observation under a stereoscopic microscope.

Transient gene expression analysis using mesophyll protoplasts

Protoplasts isolated from the first leaves of 3-week-old plants were used for DNA transfection assays to characterise subcellular localisation, as has been previously described (Wu et al., 2009; Yoo et al., 2007).

References

Aida, M., Vernoux, T., Furutani, M., Traas, J. and Tasaka, M. (2002). Roles of *PIN-FORMED1* and *MONOPTEROS* in pattern formation of the apical region of the *Arabidopsis* embryo. *Development* **129**, 3965-3974.

Anastasiou, E., Kenz, S., Gerstung, M., MacLean, D., Timmer, J., Fleck, C. and Lenhard, M. (2007). Control of plant organ size by *KLUH/CYP78A5*-dependent intercellular signaling. *Dev. Cell* **13**, 843-856.

Baud, S., Bellec, Y., Miquel, M., Bellini, C., Caboche, M., Lepiniec, L., Faure, J. D. and Rochat, C. (2004). *gurke* and *pasticcino3* mutants affected in embryo development are impaired in acetyl-CoA carboxylase. *EMBO Rep.* **5**, 515-520.

Bellec, Y., Harrar, Y., Butaeye, C., Darnet, S., Bellini, C. and Faure, J. D. (2002). *Pasticcino2* is a protein tyrosine phosphatase-like involved in cell proliferation and differentiation in *Arabidopsis*. *Plant J.* **32**, 713-722.

Benková, E., Michniewicz, M., Sauer, M., Teichmann, T., Seifertová, D., Jürgens, G. and Friml, J. (2003). Local, efflux-dependent auxin gradients as a common module for plant organ formation. *Cell* **115**, 591-602.

Bulusu, V., Prior, N., Snaebjornsson, M. T., Kuehne, A., Sonnen, K. F., Kress, J., Stein, F., Schultz, C., Sauer, U. and Aulehla, A. (2017). Spatiotemporal analysis of a glycolytic activity gradient linked to mouse embryo mesoderm development. *Dev. Cell* **40**, 331-341.

Carey, B. W., Finley, L. W. S., Cross, J. R., Allis, C. D. and Thompson, C. B. (2015). Intracellular α-ketoglutarate maintains the pluripotency of embryonic stem cells. *Nature* **518**, 413-416.

Catella, F., Lawson, J. A., Fitzgerald, D. J. and FitzGerald, G. A. (1990). Endogenous biosynthesis of arachidonic acid epoxides in humans: increased formation in pregnancy-induced hypertension. *Proc. Natl. Acad. Sci. USA* **87**, 5893-5897.

Dai, X., Wang, G., Yang, D. S., Tang, Y., Broun, P., Marks, M. D., Sumner, L. W., Dixon, R. A. and Zhao, P. X. (2010). TrichOME: a comparative omics database for plant trichomes. *Plant Physiol.* **152**, 44-54.

Diener, A. C., Li, H., Zhou, W.-X., Whoriskey, W. J., Nes, W. D. and Fink, G. R. (2000). *STEROL METHYLTRANSFERASE 1* controls the level of cholesterol in plants. *Plant Cell* **12**, 853-870.

Ebine, K., Okatani, Y., Uemura, T., Goh, T., Shoda, K., Niihama, M., Morita, M. T., Spitzer, C., Otegui, M. S., Nakano, A. et al. (2008). A SNARE complex unique to seed plants is required for protein storage vacuole biogenesis and seed development of *Arabidopsis thaliana*. *Plant Cell* **20**, 3006-3021.

Ehlting, J., Sauveplane, V., Olry, A., Ginglinger, J.-F., Provart, N. J. and Werck-Reichhart, D. (2008). An extensive (co-)expression analysis tool for the cytochrome P450 superfamily in *Arabidopsis thaliana*. *BMC Plant Biol.* **8**, 47.

Fang, W., Wang, Z., Cui, R., Li, J. and Li, Y. (2012). Maternal control of seed size by *EOD3/CYP78A6* in *Arabidopsis thaliana*. *Plant J.* **70**, 929-939.

Friml, J., Vieten, A., Sauer, M., Weijers, D., Schwarz, H., Hamann, T., Offringa, R. and Jürgens, G. (2003). Efflux-dependent auxin gradients establish the apical-basal axis of *Arabidopsis*. *Nature* **426**, 147-153.

Furutani, M., Vernoux, T., Traas, J., Kato, T., Tasaka, M. and Aida, M. (2004). *PIN-FORMED1* and *PINOID* regulate boundary formation and cotyledon development in *Arabidopsis* embryogenesis. *Development* **131**, 5021-5030.

Ginglinger, J.-F., Boachon, B., Hofer, R., Paetz, C., Kollner, T. G., Miesch, L., Lugan, R., Baltenweck, R., Mutterer, J., Ullmann, P. et al. (2013). Gene coexpression analysis reveals complex metabolism of the monoterpene alcohol linalool in *Arabidopsis* flowers. *Plant Cell* **25**, 4640-4657.

Grebe, M., Xu, J., Mobius, W., Ueda, T., Nakano, A., Geuze, H. J., Rook, M. B. and Scheres, B. (2003). *Arabidopsis* sterol endocytosis involves actin-mediated trafficking via ARA6-positive early endosomes. *Curr. Biol.* **13**, 1378-1387.

Haberer, G., Erschadi, S. and Torres-Ruiz, R. F. (2002). The Arabidopsis gene *PEPINO/PASTICCINO2* is required for proliferation control of meristematic and non-meristematic cells and encodes a putative anti-phosphatase. *Dev. Genes Evol.* **212**, 542-550.

Han, S. and Kim, D. (2006). AtRTPrimer: database for Arabidopsis genome-wide homogeneous and specific RT-PCR primer-pairs. *BMC Bioinformatics* **7**, 179.

Herridge, R. P., Day, R. C., Baldwin, S. and Macknight, R. C. (2011). Rapid analysis of seed size in *Arabidopsis* for mutant and QTL discovery. *Plant Methods* **7**, 3.

Hirai, M. Y., Yano, M., Goodenowe, D. B., Kanaya, S., Kimura, T., Awazuhara, M., Arita, M., Fujiwara, T. and Saito, K. (2004). Integration of transcriptomics and metabolomics for understanding of global responses to nutritional stresses in *Arabidopsis thaliana*. *Proc. Natl. Acad. Sci. USA* **101**, 10205-10210.

Hirai, M. Y., Sugiyama, K., Sawada, Y., Tohge, T., Obayashi, T., Suzuki, A., Araki, R., Sakurai, N., Suzuki, H., Aoki, K. et al. (2007). Omics-based identification of *Arabidopsis* Myb transcription factors regulating aliphatic glucosinolate biosynthesis. *Proc. Natl. Acad. Sci. USA* **104**, 6478-6483.

Hou, C. T. and Forman, R. J. (2000). Growth inhibition of plant pathogenic fungi by hydroxy fatty acids. *J. Indust. Microbiol. Biotech.* **24**, 275-276.

Ideker, T., Thorsson, V., Ranish, J. A., Christmas, R., Buhler, J., Eng, J. K., Bumgarner, R., Goodlett, D. R., Aebersold, R. and Hood, L. (2001). Integrated genomic and proteomic analyses of a systematically perturbed metabolic network. *Science* **292**, 929-934.

Imaishi, H., Matsuo, S., Swai, E. and Ohkawa, H. (2000). CYP78A1 preferentially expressed in developing inflorescences of *Zea mays* encoded a cytochrome P450-dependent lauric acid 12-monooxygenase. *Biosci. Biotechnol. Biochem.* **64**, 1696-1701.

Ito, T. and Meyerowitz, E. M. (2000). Overexpression of a gene encoding a cytochrome P450, *CYP78A9*, induces large and seedless fruit in *Arabidopsis*. *Plant Cell* **12**, 1541-1550.

Kajiwara, T., Furutani, M., Hibara, K. and Tasaka, M. (2004). The *GURKE* gene encoding an acetyl-CoA carboxylase is required for partitioning the embryo apex into three subregions in *Arabidopsis*. *Plant Cell Physiol.* **45**, 1122-1128.

Kawade, K., Horiguchi, G. and Tsukaya, H. (2010). Non-cell-autonomously coordinated organ size regulation in leaf development. *Development* **137**, 4221-4227.

Kawade, K., Horiguchi, G., Usami, T., Hirai, M. Y. and Tsukaya, H. (2013). ANGUSTIFOLIA3 signaling coordinates proliferation between clonally distinct cells in leaves. *Curr. Biol.* **23**, 788-792.

Keurentjes, J. J. B. (2009). Genetical metabolomics: closing in on phenotypes. *Curr. Opin. Plant Biol.* **12**, 223-230.

Kim, T.-W., Hwang, J. Y., Kim, Y. S., Joo, S. H., Chang, S. C., Lee, J. S., Takatsuto, S. and Kim, S. K. (2005). *Arabidopsis* CYP85A2, a cytochrome P450, mediates the Baeyer-Villiger oxidation of castasterone to brassinolide in brassinosteroid biosynthesis. *Plant Cell* **17**, 2397-2412.

Kuromori, T., Wada, T., Kamiya, A., Yuguchi, M., Yokouchi, T., Imura, Y., Takabe, H., Sakurai, T., Akiyama, K., Hirayama, T. et al. (2006). A trial of phenome analysis using 4000 *Ds*-insertional mutants in gene-coding regions of *Arabidopsis*. *Plant J.* **47**, 640-651.

Larkin, J. C. (1994). Isolation of a cytochrome P450 homologue preferentially expressed in developing inflorescences of *Zea mays*. *Plant Mol. Biol.* **25**, 343-353.

Li-Beisson, Y., Pollard, M., Sauveplane, V., Pinot, F., Ohlrogge, J. and Beisson, F. (2009). Nanoridges that characterize the surface morphology of flowers require the synthesis of cutin polyester. *Proc. Natl. Acad. Sci. USA* **106**, 22008-22013.

Malitsky, S., Blum, E., Less, H., Venger, I., Elbaz, M., Morin, S., Eshed, Y. and Aharoni, A. (2008). The transcript and metabolite networks affected by the two clades of *Arabidopsis* glucosinolate biosynthesis regulators. *Plant Physiol.* **148**, 2021-2049.

Miyazawa, H., Yamaguchi, Y., Sugiura, Y., Honda, K., Kondo, K., Matsuda, F., Yamamoto, T., Suematsu, M. and Miura, M. (2017). Rewiring of embryonic glucose metabolism via suppression of PFK-1 and aldolase during mouse chorioallantoic branching. *Development* **144**, 63-73.

Miyoshi, K., Ahn, B.-O., Kawakatsu, T., Ito, Y., Itoh, J.-I., Nagato, Y. and Kurata, N. (2004). *PLASTOCHRON1*, a timekeeper of leaf initiation in rice, encodes cytochrome P450. *Proc. Natl. Acad. Sci. USA* **101**, 875-880.

Mizutani, M. and Ohta, D. (2010). Diversification of P450 genes during land plant evolution. *Annu. Rev. Plant Biol.* **61**, 291-315.

Morohashi, K., Casas, M. I., Falcone Ferreyra, M. L., Mejia-Guerra, M. K., Pourcel, L., Yilmaz, A., Feller, A., Carvalho, B., Emiliani, J., Rodriguez, E. et al. (2012). A genome-wide regulatory framework identifies maize pericarp color1 controlled genes. *Plant Cell* **24**, 2745-2764.

Nakagawa, T., Kurose, T., Hino, T., Tanaka, K., Kawamukai, M., Niwa, Y., Toyooka, K., Matsuoka, K., Jinbo, T. and Kimura, T. (2007). Development of series of gateway binary vectors, pGWBs, for realizing efficient construction of fusion genes for plant transformation. *J. Biosci. Bioeng.* **104**, 34-41.

Nakamoto, M., Schmit, A.-C., Heintz, D., Schaller, H. and Ohta, D. (2015). Diversification of sterol methyltransferase enzymes in plants and a role for β-sitosterol in oriented cell plate formation and polarized growth. *Plant J.* **84**, 860-874.

Nelson, D. and Werck-Reichhart, D. (2011). A P450-centric view of plant evolution. *Plant J.* **66**, 194-211.

Notaguchi, M., Abe, M., Kimura, T., Daimon, Y., Kobayashi, T., Yamaguchi, A., Tomita, Y., Dohi, K., Mori, M. and Araki, T. (2008). Long-distance, graft-transmissible action of *Arabidopsis* FLOWERING LOCUS T protein to promote flowering. *Plant Cell Physiol.* **49**, 1645-1658.

Oginuma, M., Moncuquet, P., Xiong, F., Karoly, E., Chal, J., Guevorkian, K. and Pourquié, O. (2017). A gradient of glycolytic activity coordinates FGF and Wnt signaling during elongation of the body axis in Amniote embryos. *Dev. Cell* **40**, 342-353.

Pinot, F. and Beisson, F. (2011). Cytochrome P450 metabolizing fatty acids in plants: characterization and physiological roles. *FEBS J.* **278**, 195-205.

Reintanz, B., Lehnen, M., Reichelt, M., Gershenzon, J., Kowalczyk, M., Sandberg, G., Godde, M., Uhl, R. and Palme, K. (2001). *Bus*, a bushy *Arabidopsis CYP79F1* knockout mutant with abolished synthesis of short-chain aliphatic glucosinolates. *Plant Cell* **13**, 351-367.

Robert, H. S., Grones, P., Stepanova, A. N., Robles, L. M., Lokerse, A. S., Alonso, J. M., Weijers, D. and Friml, J. (2013). Local auxin sources orient the apical-basal axis in *Arabidopsis* embryos. *Curr. Biol.* **23**, 2506-2512.

Roman, R. J. (2002). P-450 metabolites of arachidonic acid in the control of cardiovascular function. *Physiol. Rev.* **82**, 131-185.

Roudier, F., Gissot, L., Beaudoin, F., Haslam, R., Michaelson, L., Marion, J., Molino, D., Lima, A., Bach, L., Morin, H. et al. (2010). Very-long-chain fatty acids are involved in polar auxin transport and developmental patterning in *Arabidopsis*. *Plant Cell* **22**, 364-375.

Saito, K., Hirai, M. Y. and Yonekura-Sakakibara, K. (2008). Decoding genes with coexpression networks and metabolomics - 'majority report by precogs'. *Trends Plant Sci.* **13**, 36-43.

Sauveplane, V., Kandel, S., Kastner, P. E., Ehlting, J., Compagnon, V., Werck-Reichhart, D. and Pinot, F. (2009). *Arabidopsis thaliana* CYP77A4 is the first cytochrome P450 able to catalyze the epoxidation of free fatty acids in plants. *FEBS J.* **276**, 719-735.

Schrick, K., Mayer, U., Martin, G., Bellini, C., Kuhnt, C., Schmidt, J. and Jürgens, G. (2002). Interactions between sterol biosynthesis genes in embryonic development of *Arabidopsis*. *Plant J.* **31**, 61-73.

Schuler, M. A. and Werck-Reichhart, D. (2003). Functional genomics of P450s. *Annu. Rev. Plant Biol.* **54**, 629-667.

Sciacovelli, M., Gonçalves, E., Johnson, T. I., Zecchini, V. R., da Costa, A. S. H., Gaude, E., Drubbel, A. V., Theobald, S. J., Abbo, S. R., Tran, M. G. B. et al. (2016). Fumarate is an epigenetic modifier that elicits epithelial-to-mesenchymal transition. *Nature* **537**, 544-547.

Shang, B., Xu, C., Zhang, X., Cao, H., Xin, W. and Hu, Y. (2016). Very-long-chain fatty acids restrict regeneration capacity by confining pericycle competence for callus formation in *Arabidopsis*. *Proc. Natl. Acad. Sci. USA* **113**, 5101-5106.

Stepanova, A. N., Robertson-Hoyt, J., Yun, J., Benavente, L. M., Xie, D.-Y., Doležal, K., Schlereth, A., Jürgens, G. and Alonso, J. M. (2008). TAA1-mediated auxin biosynthesis is essential for hormone crosstalk and plant development. *Cell* **133**, 177-191.

Teleman, A. A. (2016). Metabolism meets development at Wiston House. *Development* **143**, 3045-3049.

Toyoda, T. and Wada, A. (2004). Omic space: coordinate-based integration and analysis of genomic phenomic interactions. *Bioinformatics* **20**, 1759-1765.

Toyokura, K., Watanabe, K., Oiwaka, A., Kusano, M., Tameshige, T., Tatematsu, K., Matsumoto, N., Tsugeki, R., Saito, K. and Okada, K. (2011). Succinic semialdehyde dehydrogenase is involved in the robust patterning of *Arabidopsis* leaves along the adaxial-abaxial axis. *Plant Cell Physiol.* **52**, 1340-1353.

Treml, B. S., Winderl, S., Radykewicz, R., Herz, M., Schweizer, G., Hutzler, P., Glawischnig, E. and Torres Ruiz, R. A. (2005). The gene *ENHANCER OF PINOID* controls cotyledon development in the *Arabidopsis* embryo. *Development* **132**, 4063-4074.

Tsuge, T., Tsukaya, H. and Uchimiya, H. (1996). Two independent and polarized processes of cell elongation regulate leaf blade expansion in *Arabidopsis thaliana* (L.) Heynh. *Development* **122**, 1589-1600.

Tsukagoshi, H., Busch, W. and Benfey, P. N. (2010). Transcriptional regulation of ROS controls transition from proliferation to differentiation in the root. *Cell* **143**, 606-616.

Willemsen, V., Friml, J., Grebe, M., van den Toorn, A., Palme, K. and Scheres, B. (2003). Cell polarity and PIN protein positioning in *Arabidopsis* require *STEROL METHYLTRANSFERASE1* function. *Plant Cell* **15**, 612-625.

Wilson-Sánchez, D., Rubio-Díaz, S., Muñoz-Viana, R., Pérez-Pérez, J. M., Jover-Gil, S., Ponce, M. R. and Micol, J. L. (2014). Leaf phenomics: a systematic reverse genetic screen for *Arabidopsis* leaf mutants. *Plant J.* **79**, 878-891.

Winter, D., Vinegar, B., Nahal, H., Ammar, R., Wilson, G. V. and Provart, N. J. (2007). An "Electronic Fluorescent Pictograph" browser for exploring and analyzing large-scale biological data sets. *PLoS ONE* **2**, e718.

Wu, F. H., Shen, S. C., Lee, L. Y., Lee, S. H., Chan, M. T. and Lin, C. S. (2009). Tape-*Arabidopsis* Sandwich - a simpler *Arabidopsis* protoplast isolation method. *Plant Methods* **5**, 16.

Xu, J., Hofhuis, H., Heidstra, R., Sauer, M., Friml, J. and Scheres, B. (2006). A molecular framework for plant regeneration. *Science* **311**, 385-388.

Yonekura-Sakakibara, K., Tohge, T., Matsuda, F., Nakabayashi, R., Takayama, H., Niida, R., Watanabe-Takahashi, A., Inoue, E. and Saito, K. (2008). Comprehensive flavonol profiling and transcriptome coexpression analysis leading to decoding gene-metabolite correlations in *Arabidopsis*. *Plant Cell* **20**, 2160-2176.

Yoo, S. D., Cho, Y. H. and Sheen, J. (2007). *Arabidopsis* mesophyll protoplasts: a versatile cell system for transient gene expression analysis. *Nat. Protoc.* **2**, 1565-1572.

Zeldin, D. C., Moomaw, C. R., Jesse, N., Tomer, K. B., Beetham, J., Hammock, B. D. and Wu, S. (1996). Biochemical characterization of the human liver cytochrome P450 arachidonic acid epoxygenase pathway. *Arch. Biochem. Biophys.* **330**, 87-96.